CALIBRATION OF CONSTANT ANGULAR ERROR FOR CBERS-2 IMAGERY WITH FEW GROUND CONTROL POINTS

Junpeng YU [a, *] Xiuxiao YUAN [a] Zhenli WU [a]

[a] School of Remote Sensing and Information Engineering, Wuhan University, Wuhan, China 430079
strength701@126.com

Commission I, WG I/5

KEY WORDS: Spaceborne remote sensing, High-resolution image, Space photogrammetry, Calibration, Process modelling, Accuracy

ABSTRACT:

The rigorous geometric model which depends on physical properties of the image acquisition is the basic model for object positioning of high resolution satellite imagery (HRSI). Using the linear and angular elements provided by ephemeris and attitude measuring system carried on the satellite, the object coordinates can be determined by the rigorous geometric model when the image coordinates are given. Although attitude data measuring instruments have been improved in recent years, the precision of original attitude data acquired can hardly satisfy the requirement of direct georeferencing. For direct georeferencing application of CBERS-2 satellites developed independently in China, the ephemeris data are provided by MPSS (mission planning and supporting system) and GPS. The attitude data are provided by star sensor. After post-pass data processing, the error of ephemeris can be controlled within 20 meters, while the errors of attitude angles in all three axes (pitch, roll, and yaw) exceed 50 arc seconds.In this paper, the rigorous geometric model suited for CBERS-2 satellites containing a series of reference coordinate transformation is first introduced. The direct georeferencing results show that location root mean square error is more than 1000 meters for planimetry, the main part of which is systematic error caused by constant angular error (CAE). On the basis of the experiment analysis, a calibration model for eliminating constant angular error for CBERS-2 imagery is established. The calibration model can be easily realized and requires only few ground control points (GCPs).The calibration model has been tested on two scenes of CBERS-2 imagery. In each test, various numbers of GCPs have been used to calculate the CAE and the distinction of the results is subtle. Due to the sufficient SNR of CBERS-2 attitude data, the calibration model is able to reduce the location error to 50~65 meters for planimetry by single GCP, nearly 95 percent improvement to original result. It is significantly efficient especially under the situation of lack of GCPs. Further more, after calibrating the initial attitude, the model can provide refined initial angular elements for the following photogrammetry mission such as space resection and bundle adjustment of the imagery when enough GCPs are available.

1. INTRODUCTION

With the fast development of spacecraft manufacturing and spaceborne optics, space sensors have provided new and efficient data sources for observing the surface of the earth. Compared with aerial photogrammetry, high resolution satellite imagery (HRSI) is faster, cheaper, more efficient and with a larger swath width. In the defence applications, HRSI plays an important role in intelligence gathering, change detection, precise mapping and target navigation and so on. Whereas in civilian area, HRSI makes also contributions to mapping, construction, mining, urban planning, land use investigation, resource management, agricultural survey, environment monitoring and GIS serve. Therefore in many countries, high resolution remotely sensed satellites are positively developed and launched. Among them, IKONOS, QuickBird and SPOT series are the typical examples of commercial high resolution remotely sensed satellites (Zhang, 2004). The best ground sampling distance (GSD) has achieved sub-meter. In China, CBERS-2 series of satellites, which are developed independently, have been successfully running since 2000. CBERS-2-2 and CBERS-2-3 are equipped with high resolution pushbroom sensors, in which the linear array is fabricated by 4 pieces of CCD segments aligned within the focal plane. The best GSD at nadir point achieves 3 meters.

In order to establish the geometric relationship between image coordinates and the corresponding ground coordinates, the accurate linear and angular orientation elements must be retrieved at first. In aerial photogrammetry, we can calculate the orientation elements with space resection method using at least 3 GCPs. In space photogrammetry, however, the similar process is much more difficult due to the complicated imaging geometry. Furthermore, to ensure the accuracy and reliability of the orientation result, enough quantity and suitable distribution of GCPs are strictly required.

For such reasons, at present most of the high resolution remotely sensed satellites carry high-precision orbit positioning and attitude measuring system onboard to provide direct measurement of the sensor orientation elements. On CBERS-2 satellites, MPSS (mission planning and supporting system) and GPS (global positioning system) can provide the sensor position while star sensors provide the sensor attitude at certain instants of time. This information, together with suitable interpolation techniques, may be used to calculate the sensor position and attitude for any particular instants of acquisition and apply direct georeferencing. This method does not require any GCPs, except for final checking, but the effectiveness and reliability of this method depend on the accuracy of the available orientation

* Corresponding author.

elements. A great number of direct georeferencing experiments with CBERS-2 imagery have shown that location accuracy of CBERS-2 imagery is about 800 meters or even worse. Comparing to the French satellite SPOT-5 which has a similar GSD of 2.5 meters and the location accuracy of 50 meters, the performance of CBERS-2 imagery is far from expectation. When not considering terrain undulation, root mean square error (RMSE) locating the object point with CBERS-2 imagery vary between 600 meters to 1100 meters for planimetry.

According to official public information, after post-pass data processing the direct measuring error of orbit positioning can be controlled within 20 meters, which has relatively little effect on the result of direct georeferencing. Obviously, the major location error is caused by systematic errors of the original attitude data. Relative researches have shown that the main part of systematic error is constant error, which should be separated at first (Wang, 2002). Therefore, it is of great importance to effectively eliminate the constant angular error (CAE) .In this paper, the rigorous geometric model suited for CBERS-2 satellites including a series of coordinate transformation is introduced firstly. The direct georeferencing tests on CBERS-2 imagery with rigorous model confirm the existence of the CAE. Then a new method for calibrating the CAE with few GCP is established. After compensating the CAE, the RMSE of direct georeferencing has been improved sufficiently.

2. RIGOROUS GEOMETRIC MODEL

2.1 Collinearity equation

Collinearity equation is the rigorous geometric model for direct georeferencing of HRSI and the basic model for HRSI geometric processing (Poli, 2002). In order to eliminate the complicated distortion effect caused by earth curvature and self-rotation, earth centred rotating coordinate system (ECR) such as WGS-84 is always adopted as the object space coordinate system in rigorous metric model. For convenience of coordinate transformation from an image point to its corresponding ground point, the space auxiliary coordinate system is defined with the perspective centre as the origin and three axes parallel to those of the ECR. The rigorous geometric model is first to calculate the space auxiliary coordinate through a series of coordinate transformation (Yuan, 2003). The process can be expressed as:

$$\begin{bmatrix} X_M - X_{P_i} \\ Y_M - Y_{P_i} \\ Z_M - Z_{P_i} \end{bmatrix} = \lambda \boldsymbol{SRT} \begin{bmatrix} x_i \\ 0 \\ -f \end{bmatrix} \tag{1}$$

Where, $\boldsymbol{\mu}_m = \boldsymbol{SRT}\begin{bmatrix} x_i & 0 & -f \end{bmatrix}^{\mathrm{T}}$ are the auxiliary coordinate of image point i, $\boldsymbol{\mu}_S = \dfrac{\boldsymbol{\mu}_m}{\|\boldsymbol{\mu}_m\|}$ are the normalized coordinates of $\boldsymbol{\mu}_m$; (X_M, Y_M, Z_M) are space coordinates of the ground point in ECR. $(X_{P_i}, Y_{P_i}, Z_{P_i})$ are space coordinates of the perspective centre for image point i; λ is the scale element; $\boldsymbol{S}$ is the transformation matrix for converting the satellite orbit coordinates to ECR coordinates; $\boldsymbol{T}$ is the transformation matrix for converting the sensor coordinates to the satellite body coordinates; $\boldsymbol{R}$ is the transformation matrix for converting the satellite body coordinates to the orbit coordinates, and it can be anatomized as :

$$\boldsymbol{R} = \boldsymbol{R}_\omega \boldsymbol{R}_\varphi \boldsymbol{R}_\kappa \tag{2}$$

where,

$$\boldsymbol{R}_\omega = \begin{bmatrix} 1 & 0 & 0 \\ 0 & \cos\omega_i & \sin\omega_i \\ 0 & -\sin\omega_i & \cos\omega_i \end{bmatrix},$$

$$\boldsymbol{R}_\varphi = \begin{bmatrix} \cos\varphi_i & 0 & -\sin\varphi_i \\ 0 & 1 & 0 \\ \sin\varphi_i & 0 & \cos\varphi_i \end{bmatrix},$$

$$\boldsymbol{R}_\kappa = \begin{bmatrix} \cos\kappa_i & -\sin\kappa_i & 0 \\ \sin\kappa_i & \cos\kappa_i & 0 \\ 0 & 0 & 1 \end{bmatrix}.$$

Where, $\omega_i, \varphi_i, \kappa_i$ are respectively the pitch, roll, yaw angle of the scan line i. It is important to note that S and R are both dependent on scan time while T is determined by the position of the image point in the linear sensor. All of them are orthogonal transformation matrixes.

CBERS-2 satellites use CCD linear array sensors, which generate 2D imagery in the pushbroom mode. Due to the stability of the satellite trajectory, the motion of the perspective point and the change of the attitude can be expressed by multi-order polynomial functions as (Poli, 2004):

$$\begin{cases} X_{P_i} = a_0 + a_1 t + a_2 t^2 + \cdots\cdots + a_k t^k \\ Y_{P_i} = b_0 + b_1 t + b_2 t^2 + \cdots\cdots + b_k t^k \\ Z_{P_i} = c_0 + c_1 t + c_2 t^2 + \cdots\cdots + c_k t^k \\ \omega_i = d_0 + d_1 t + d_2 t^2 + \cdots\cdots + d_k t^k \\ \varphi_i = e_0 + e_1 t + e_2 t^2 + \cdots\cdots + e_k t^k \\ \kappa_i = f_0 + f_1 t + f_2 t^2 + \cdots\cdots + f_k t^k \end{cases} \tag{3}$$

Where, $a_0, b_0, c_0, d_0, e_0, f_0$ are the orientation elements of the centre scan line; $a_1, \cdots\cdots, f$ are the coefficients of the polynomials and they can be computed by the discrete ephemeris and attitude observation values provided in metadata file. The reference (Song, 2003) indicates that the fitting error is no more than 0.25 meters for linear elements and 0.1 arc second for angular elements when the order is 4 or above.

2.2 The principle of image georeferencing

Georeferencing of the remote-sensing imagery is actually to obtain the intersection point of the imaging ray with the earth surface. Fig (1) shows the intersection point graphically.

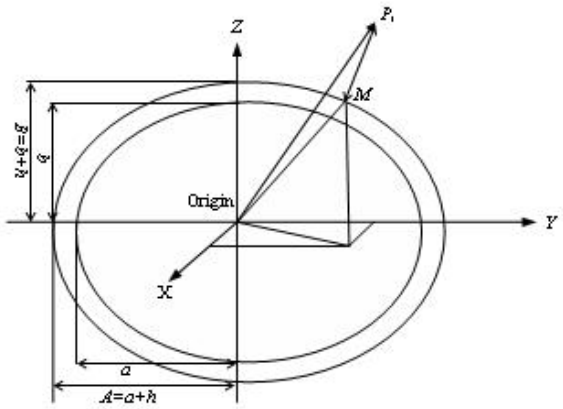

Figure.1 Intersection of look direction with the Earth ellipsoid

After determining the look direction of the imaging ray in ECR system, we have:

$$\begin{cases} X_M = X_{P_i} + \lambda(\boldsymbol{\mu}_S)_X \\ Y_M = Y_{P_i} + \lambda(\boldsymbol{\mu}_S)_Y \\ Z_M = Z_{P_i} + \lambda(\boldsymbol{\mu}_S)_Z \end{cases} \tag{4}$$

Another available condition is the ellipsoid equation of the earth:

$$\frac{X_M^2 + Y_M^2}{A^2} + \frac{Z_M^2}{B^2} = 1 \tag{5}$$

in which $A = a + h; B = b + h$ and a, b are the semiaxle lengths of the Earth ellipsoid. h is the ellipsoid height that can be assumed as rough value when no terrain data available. If DEM is available, the ellipsoid height can be retrieved from DEM through an iterative process. Combining equations (4) and (5), we can extract the quadratic equation as below:

$$\begin{aligned} &(\frac{(\boldsymbol{\mu}_S)_X^2 + (\boldsymbol{\mu}_S)_Y^2}{A^2} + \frac{(\boldsymbol{\mu}_S)_Z^2}{B^2})\lambda^2 + \\ &2(\frac{X_{P_i}(\boldsymbol{\mu}_S)_X + Y_{P_i}(\boldsymbol{\mu}_S)_Y}{A^2} + \\ &\frac{Z_{P_i}(\boldsymbol{\mu}_S)_Z}{B^2})\lambda + (\frac{X_{P_i}^2 + Y_{P_i}^2}{A^2} + \frac{Z_{P_i}^2}{B^2}) = 1 \end{aligned} \tag{6}$$

It is obvious that two theoretic solutions of λ can be obtained from equations (6) but just one of them is the actual solution. A simple method is to put both two solutions into equation (4) and the one which makes the corresponding (X_M, Y_M, Z_M) more close to $(X_{P_i}, Y_{P_i}, Z_{P_i})$ is the actual solution.

3. CALIBRATION OF CONSTANT ANGULAR ERROR FOR CBERS2

3.1 Error of the observed attitudes

Though the attitude measuring instruments such as star sensor has been improved for recent years, its precision can not satisfy the requirement of direct georeferencing for HRSI. Actually, the precision of star sensor is determined by visual angle、focal length、the number and distribution of the distinguished stars in measuring time. In many cases the number of stars is insufficient or they don't evenly distribute in the view field, which leads to the difference between real precision and theory precision. Consequently, the uncertainty of the values of observed attitudes becomes the major cause of location error. The traditional method to refine the initial observations is least-squares adjustment but it requires a certain number of GCPs in the target area. For much area in short of GCPs such as the west region of China, we have to search alternative method to improve the georeferencing accuracy.

Due to the major part of the attitude error is constant, an simple way to reduce the location error is eliminating the constant attitude error (CAE) by few GCPs. For there exist obvious CAE in the original attitude observations, this method is very efficient and practicable.

3.2 Mathematical model for calibrating CAE

Given the sensor coordinates (x_c, y_c) of any single image point and its corresponding ground point (X_c, Y_c, Z_c), we can calculate the position of the corresponding perspective centre $(X_{P_i}, Y_{P_i}, Z_{P_i})$ and the original attitude value $(\omega_i^0, \varphi_i^0, \kappa_i^0)$ by equation (3). When the accuracy of $(X_{P_i}, Y_{P_i}, Z_{P_i})$ and (X_c, Y_c, Z_c) is high enough, $\boldsymbol{\mu}_c$ in equation (7) can be regarded as the exact look direction of the imaging ray, which constitutes the prerequisite condition for detecting CAE:

$$\boldsymbol{\mu}_c = \frac{\boldsymbol{\mu}_c'}{\|\boldsymbol{\mu}_c'\|} \tag{7}$$

where,

$$\boldsymbol{\mu}_c' = \begin{bmatrix} X_c - X_{P_i} \\ Y_c - Y_{P_i} \\ Z_c - Z_{P_i} \end{bmatrix}$$

According to equation (4) we have:

$$\boldsymbol{\mu}_c = \boldsymbol{\mu}_S \tag{8}$$

For any single control point, three observation equations can be constructed by linearizing Eq. (8).

$$\boldsymbol{V} = \begin{bmatrix} V_X \\ V_Y \\ V_Z \end{bmatrix} = \begin{bmatrix} \frac{\partial(\boldsymbol{\mu}_S)}{\partial\omega_i} & \frac{\partial(\boldsymbol{\mu}_S)}{\partial\varphi_i} & \frac{\partial(\boldsymbol{\mu}_S)}{\partial\kappa_i} \end{bmatrix} \begin{bmatrix} \Delta\omega_i \\ \Delta\varphi_i \\ \Delta\kappa_i \end{bmatrix} - \boldsymbol{L} \quad (9)$$

Where,

$\boldsymbol{L} = \begin{bmatrix} (\boldsymbol{\mu}_c)_X - (\boldsymbol{\mu}_S)_X \\ (\boldsymbol{\mu}_c)_Y - (\boldsymbol{\mu}_S)_Y \\ (\boldsymbol{\mu}_c)_Z - (\boldsymbol{\mu}_S)_Z \end{bmatrix}$ is the residuals vector between $\boldsymbol{\mu}_c$ and $\boldsymbol{\mu}_S$.

In equation (9), $(\omega_i^0, \varphi_i^0, \kappa_i^0)$ are used as initial values and the correction vector $(\Delta\omega_i, \Delta\varphi_i, \Delta\kappa_i)$ can be obtained by least-squares estimation. The calibrated attitude are assumed to be $(\omega_i^0 + \Delta\omega_i, \varphi_i^0 + \Delta\varphi_i, \kappa_i^0 + \Delta\kappa)$ .By 3~4 times of iteration calculating, the values of $(\Delta\omega_i, \Delta\varphi_i, \Delta\kappa_i)$ become ignorable and the iteration stopped.

3.3 Computing CAE with few GCPs

When original observed attitudes containing constant angular error, the error can be estimated with few GCPs. For there exists the same constant error for each scan line in one image scene, correction vector $(\Delta\omega_i, \Delta\varphi_i, \Delta\kappa_i)$ obtained by the way introduced in §3.2 can be taken as the CAE if only one GCP available; When n GCPs in n scan lines have been measured, for each scan line we can obtain their corresponding correction attitudes and a more reliable CAE can be obtained by computing their mean value, such as equation (10) expressed:.

$$\begin{cases} \Delta\omega = \frac{1}{n}\sum_{i=1}^{n}\Delta\omega_i \\ \Delta\varphi = \frac{1}{n}\sum_{i=1}^{n}\Delta\varphi_i \\ \Delta\kappa = \frac{1}{n}\sum_{i=1}^{n}\Delta\kappa_i \end{cases} \quad (10)$$

After compensating CAE for the original observed attitudes, the precision of the attitude is sufficiently improved. However, there must be random errors remained in the calibrated attitudes, which can be removed by further adjustment way such as space resection method when at least 6 GCPs are available .

4. TEST AND RESULT ANALYSIS

In order to prove the existence of the CAE and the efficiency of above calibration method, two scenes of CBERS2 imagery have been tested.

Scene1 is acquired on Nov17 of 2004. Scene2 is acquired on Dec7 of 2004.The sizes of both images are 10002pixels×10000pixels and the processing level are level1, i.e." stitched raw" image data without corrections except for the radiometric improvement. Level1 data can be processed with rigorous geometric model. The image quality of both two takes was good. No missing lines exist. Tab1 gives the results of direct georeferencing without using any GCPs.

SCENE	RMSE (m)		
	X	*Y*	*XY*
1	689.92	862.64	1104.59
2	645.06	844.51	1062.69

Table 1. Results of direct location for CBERS-2 imagery

After computing the attitude corrections by the way presented in §3.2, it is notable that the attitude corrections in all three axis distribute around certain values, which can be considered as the constant errors. The results of using different number of GCPs randomly selected to estimate the CAE for two scenes are listed at Tab2 and Tab3. It is important to note that the CAEs for different CBERS2 images are different so they should be processed independently.

GCPs	CAE (arc seconds)		
	$\Delta\omega$	$\Delta\varphi$	$\Delta\kappa$
2	-381.78	-212.93	53.34
6	-382.21	-219.41	54.81
8	-383.35	-220.72	55.59
12	-388.84	-217.93	56.55
20	-389.01	-213.70	55.63
36	-387.17	-206.41	53.15

Table 2. Constant angular error of imagery Scene1

GCPs	CAE (arc seconds)		
	$\Delta\omega$	$\Delta\varphi$	$\Delta\kappa$
2	-405.74	-189.76	12.15
6	-396.74	-194.37	11.93
8	-394.50	-196.45	12.84
12	-392.67	-195.50	12.69
20	-387.26	-210.05	12.41
27	-390.07	-213.06	13.18

Table 3. Constant angular error of imagery Scene2

For there are many complicated factors effecting location accuracy during image collecting process, the random errors do exist. If considering the CAE as signal while other random errors as noise, the estimation efficacy of CAE is determined by the SNR. When SNR is small which means that CAE is not significant compared to the random error, it will be reluctant to separate CAE. When SNR is sufficient, the CAE can be removed efficiently by even single GCP .It is very useful in the situation in short of GCPs. Tab 4 are the direct georeferencing results after compensating the CAE, Compared to Tab1, the location accuracy of SCENE1 has been improved by 95% and the location accuracy of SCENE2 has been improved by 94%. According to the corresponding resolution of the ground, the location accuracy is better than 20 pixels. In fact, the accuracy will be further improved after removing the image measuring error. The results fully show the efficiency of the calibration model to CBERS2 imagery.

SCENE	RMSE (m)		
	X	*Y*	*XY*
1	29.19	46.61	54.99
2	50.12	38.17	63.01

Table 4. Results of direct location after attitude calibration

5. CONCLUSIONS

Using the CAE calibration model presented in this paper, CAE of the CBERS2 imagery can be efficiently compensated using only one GCP. Wholly speaking, the accuracy of direct georeferencing can be improved into 20 pixels after CAE compensation. Considering that the geometric condition of single image is weaker than that of stereo images, this result is acceptable in the precision less-demanding cases. Compared to using affine transformation coefficients to model the systematic errors, the calibration method requires much less GCPs and the effect may be even better.

Although the advantages of the calibration model are obvious, the model ignores some other causes leading to location error. For example, the linear elements measured by orbit positioning system also comprise systematic error. In addition, there exist a space offset between the observed point of the positioning system and the real perspective centre. This offset is also an unknown value. Furthermore, the inner orientation elements are presumed to be precise and atmosphere refraction effect is ignored. All these factors are bound to generate location error. To better solve this problem, the more complicated adjustment models are to be investigated.

REFERENCES

Poli, D., 2002. General Model for Airborne and Spaceborne Linear Array Sensors. *International Archives of Photogrammetry and Remote Sensing*, Part B1, pp.177-182.

Poli, D., 2004. Orientation of Satellite and Airborne Imagery from Multi-Line Pushbroom Sensors with a Rigorous Sensor Model. *International Archives of Photogrammetry and Remote Sensing*,Part B1, pp.130-135.

Song Weidong, Wang Weixi, Hu Xinghua, 2003. Precise Acquisition of SPOT-5 Exterior Orientation Elements Using Metadata Data File. *Bulletin of Surveying and Mapping*, 2003(12), pp.29-31

SPOT Satellite Geometry Handbook. http://www.spotimage.fr

Wang Renxiang, 2002. EFP Aerial Triangulation of Satellite Borne Three-line Array CCD Image (II). *Science of Surveying and Mapping*, 2002 (1), pp.1-7

Yuan Xiuxiao, Zhang Guo, 2003. Object Location of Satellite under Lacking Ground Control Points. *Geomatics and Information Science of Wuhan University*, 28(5), pp.505-509

Zhang Yongsheng, Gong Danchao, et al, 2004. *Application of High-resolution Remote Sensing Satellites*. Science Press, Beijing.

ACKNOWLEDGEMENTS

Thanks for the supporting from the 973 Program of the People's Republic of China under Grant 2006CB701302 and the National Natural Science of China under Grant 407721001.